Journal of Theoretical Biology 493 (2020) 110208

Contents lists available at ScienceDirect

Journal of Theoretical Biology

journal homepage: www.elsevier.com/locate/jtb

Modeling the long term effects of thermoregulation on human sleep

Selenne Bañuelos[a,*], Janet Best[b], Gemma Huguet[c], Alicia Prieto-Langarica[d], Pamela B. Pyzza[e], Shelby Wilson[f]

[a] Department of Mathematics, California State University-Channel Islands, Camarillo, CA, United States
[b] Department of Mathematics, The Ohio State University, Columbus, OH, United States
[c] Departament de Matemàtiques, Universitat Politècnica de Catalunya, Barcelona, Spain
[d] Department of Mathematics and Statistics, Youngstown State University, Youngstown, OH, United States
[e] Department of Mathematics and Computer Science, Ohio Wesleyan University, Delaware, OH, United States
[f] Department of Biology, University of Maryland, College Park, MD, United States

ARTICLE INFO

Article history:
Received 18 January 2019
Revised 23 December 2019
Accepted 19 February 2020
Available online 19 February 2020

Keywords:
REM cycle
REM latency
Body temperature

ABSTRACT

The connection between human sleep and energy exertion has long been regarded as part of the reasoning for the need to sleep. A recent theory proposes that during REM sleep, energy utilized for thermoregulation is diverted to other relevant biological processes. We present a mathematical model of human sleep/wake regulation with thermoregulatory functions to gain quantitative insight into the effects of ambient temperature on sleep quality. Our model extends previous models by incorporating equations for the metabolic processes that control thermoregulation during sleep. We present numerical simulations that provide a quantitative answer for how humans adjust by changing the normal sleep stage progression when it is challenged with ambient temperatures away from thermoneutral. We explore the dynamics for a single night and several nights. Our results indicate that including the effects of temperature is a vital component of modeling sleep.

1. Introduction

Sleeping is one of the most important and many times overlooked physiological process in humans (Carskadon and Dement, 2011). It has been defined as a state with decreased physical motility, lack of consciousness, and with elevated sensory thresholds (Siegel, 2005). It is known and well-accepted that during sleep the body undergoes many vital processes such as storing memories, repairing muscles, neuronal network re-organization, and synthesizing proteins (Shapiro et al., 1984).

There is abundant academic and lay literature on the sleep deprivation of modern society and the effects that this lack of sleep can have on human health (Harrison and Horne, 2000; Tarawah, 2017; Borbély et al., 1981; Pasula et al., 2018; Knott et al., 2017). Studies have found strong relationships between a lack of sufficient sleep and diseases such as diabetes, obesity, high blood pressure, heart disease, among many others (Avidan, 2018; Imeri and Opp, 2009). While the effects of not sleeping have been studied for decades, the precise function of sleep has in the past evaded researchers.

Circadian-entrained healthy humans spend close to one third of their lives sleeping. Therefore, understanding the factors that affect sleep quantity and quality is vital. An important factor that can affect sleep is temperature (Harding et al., 2019; Schmidt, 2014; Schmidt et al., 2017). Humans, as well as other warm-blooded organisms have the ability to maintain a reasonable core body temperature while exposed to a fairly wide range of ambient temperatures. Thermoregulation is the process by which organisms maintain their core body temperature (Charkoudian, 2003; Romeijn et al., 2012) as the ambient temperature deviates from thermoneutrality (around 29°).

Recently published work by Schmidt presents a unifying theory of the function of sleep among all species (Schmidt, 2014). The Energy Allocation Theory hypothesizes that the function of sleep is to downregulate processes which are normally done while awake (such as foraging, mating, escaping predators) and to upregulate energy-expensive processes such as memory storage, protein synthesis, and muscle repair (Schmidt, 2014; Schmidt et al., 2017). One of the most energy-expensive processes of humans is thermoregulation (Charkoudian, 2003), which is known to be suspended during certain stages of sleep. Despite its importance and studies that conclude a strong relationship between

* Corresponding author.
E-mail addresses: selenne.banuelos@csuci.edu (S. Bañuelos), jbest@math.ohio-state.edu (J. Best), gemma.huguet@upc.edu (G. Huguet), aprietolangarica@ysu.edu (A. Prieto-Langarica), pbpyzza@owu.edu (P.B. Pyzza), shelbynwilson@umd.edu (S. Wilson).

https://doi.org/10.1016/j.jtbi.2020.110208
0022-5193/

thermoregulation and sleep, temperature remains one of the most overlooked factors when studying sleep (Romeijn et al., 2012).

Some ways in which humans maintain healthy core body temperatures are: sweating, extending their bodies, and vasodilatation to prevent overheating; shivering, vasoconstriction, and compressing their bodies to combat cold (Charkoudian, 2003). While asleep, the body loses some of its ability to thermoregulate, freeing extra energy for the processes reserved for sleep. If the body is not thermoregulating as much, body temperature will be strongly affected by the ambient temperature. For this reason, the ambient temperature at which we sleep plays a crucial role in the quantity and the quality of our sleep (Schmidt, 2014; Cheshire, 2016).

During sleep, the brain switches between two very different states: Rapid Eye Movement (REM) and Non-Rapid Eye Movement (NREM) (Carskadon and Dement, 2011). While in NREM, the human brain cortex shows slow-wave activity; the body presents decreased muscle tone and decreased ability to thermoregulate (Bassi et al., 2009). During REM, the cortex shows rapid, short-wave activity, similar to wake; the body presents a complete absence of muscle tone and an almost complete inability to thermoregulate. The significant lack of movement and thermoregulation during REM sleep frees up a large amount of energy to perform other maintenance processes, like storing memories, as described in Schmidt (2014).

Mathematical models of sleep often neglect the effects of temperature on sleep (Achermann and Borbèly, 2003), as these effects pose additional complexities to the already-intricate nature of sleep. However, given the potential impact of temperature on both the quality and quantity of human sleep, including temperature as a model feature is imperative (Van Someren, 2006; Schmidt et al., 2017; Schmidt, 2014). Thus, we have developed a mathematical model that incorporates this key component and its effects on sleep, so that we may better describe and understand the mechanisms underlying sleep behavior when thermoregulation plays a role.

In a previous paper, we developed a model of human sleep/wake and REM/NREM behaviors that incorporated the influence of ambient temperature. This model focused on producing results about the REM bout length and the number of awakenings during a night (Bañuelos et al., 2015). Due to the simplicity of the model, in which temperature deviations could only cause premature awakenings from REM sleep, we could not investigate effects such as changes in the REM latency or percentage of REM sleep. Our previous model (Bañuelos et al., 2015) only incorporated the effects of temperature onto the Preoptic Anterior Hypothalamus (POAH) neurons (which are active during sleep), a brain region critical in the thermoregulation process (Boulant, 2006; Romanovsky, 2007). The extended model proposed in this paper of the human sleep/wake system comprises neuronal populations involved in sleep/wake and REM/NREM cycles and incorporates several effects of temperature on the activation of these populations.

Furthermore, in order to incorporate the Energy Allocation Theory proposed in Schmidt (2014), the model presented here does not utilize a REM homeostat, but instead, makes use of a temperature-dependent REM regulator. This mechanism is a hypothetical instantiation of how the REM-NonREM cycle might be effected by the temperature-sensitive neurons contained in the POAH. This implementation may provide insight for experimental inquiry about the underlying connectivity between the POAH and the neurons that regulate the REM-NonREM cycle.

That is, the propensity to fall into REM sleep depends mainly on the body temperature rather than the amount of time spent in NREM sleep. Moreover, this propensity is modulated by metabolic expenditure necessary to maintain body temperature. Thus, when the body uses a lot of energy to thermoregulate, REM latency increases. This extended model allows us to study new effects of temperature on sleep rhythms, particularly on the REM bouts, and hence on sleep quality and quantity.

In Section 2.1, we present a general description of the model with details of the equations modeling the temperature effects. A complete description can be found in the Appendix. Motivated by experimental procedures in the literature, we investigate two simulation protocols, a Single Night Measurement and a Fixed Temperature Average. Detailed descriptions of these protocols are discussed in Section 2.2. Features of the model that allow temperature to affect the activity of the POAH and the temperature-dependent REM regulator are presented in Section 3.2. Model dynamics and the behavior of the model at the thermoneutral temperature of 29° are discussed in Sections 3.3 and 3.1, respectively. Results for the two simulation protocols at different temperatures are discussed in Section 3.4. Further discussion and comparison between our model and experimental results can be found in Section 4.

2. Materials and methods

2.1. Model equations

The model considered was mostly developed in Bañuelos et al. (2015) and based on a model by Kumar et al. (2012). It consists of 6 neuronal populations with directed, excitatory and inhibitory connections: the preoptic area of the hypothalamus (POAH), the brainstem reticular formation (CRF), the orexinergic neurons (ORX), the midrain reticular formation (MRF), neuron populations promoting REM sleep (Ron), and neurons that inhibit REM sleep (Roff) (see Fig. 1). The MRF and ORX are active during wake, while the CRF and POAH are active during sleep. Details concerning the neuronal populations may be found in Bañuelos et al. (2015) and Kumar et al. (2012). Here, we present additional temperature effects impacting the REM-OFF populations (represented by the blue dashed inhibitory connection in Fig. 1), which will be discussed in detail in Section 3.2.

In this section we review the basic description of the model and we refer the reader to the Appendix for more details. The model, which is based upon (Kumar et al., 2012), describes the mean activity of each neuronal population using Morris-Lecar equations (Morris and Lecar, 1981):

$$\begin{aligned} v_i' &= I_{ion,i}(v_i, w_i) + I_i - \sum I_{syn}, \\ w_i' &= \lambda_{\infty,i}(v_i)(w_{\infty,i}(v_i) - \omega_i), \end{aligned} \tag{1}$$

with $i = \{POAH, CRF, ORX, MRF, Ron, Roff\}$. Here v_i is interpreted as the mean firing rate of the ith neuronal population, and w_i is a variable representing the activation of a slow negative feedback mechanism responsible of terminating the activity episodes of a population. The term $I_{ion,i} := I_{Ca} + I_K + I_{leak}$ (see

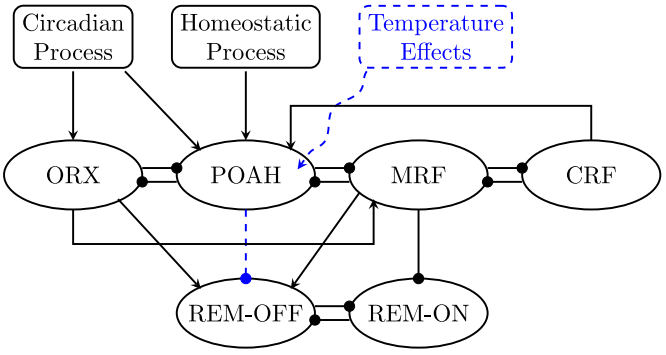

Fig. 1. Model Diagram: Temperature effects are indicated by blue dashed lines. Notice that the temperature effects go directly to the POAH but also play a role in the inhibitory connection from the POAH to the REM-OFF neuronal population.

Eq. (A.1)) represents the intrinsic population dynamics, including the mechanisms responsible of initiating and terminating the activity episodes, the latter depending on w_i. The term I_i represents the external applied current.

The term ΣI_{syn} for each population involves a specific combination of synaptic currents from neighboring populations and external sources, which can be excitatory and inhibitory. For instance, in the case of POAH, the external currents correspond to the terms $I_h(t)$ and $I_{circ}(t)$ which model the homeostatic and the circadian processes, respectively. The synaptic current from population i to population j is modeled as

$$I_{syn,i\to j} = g_{syn,i\to j} s_{\infty,i\to j}(v_i)(v_j - E_{syn,i\to j}),$$

where $g_{syn,i\to j}$ is the strength of the synapse, $E_{syn,i\to j}$ is the synaptic reversal potential and $s_{\infty,i\to j}$ is the activation function with sigmoidal shape.

The functions $w_{\infty,i}$ and $\lambda_{\infty,i}$ in Eq. (1) correspond to the steady state activation function and the rate constant function for the recovery variable w_i, respectively.

Finally, we emphasize that some functions depend directly on the body temperature T_b, namely, the activity of the *POAH* population described by v_{POAH} as well as the synaptic current $I_{POAH\to Roff}$. In turn, the body temperature T_b depends on the ambient temperature T_a and the model's ideal body temperature T_{set} (see Fig. 3), given by Eq. (A.3) as in Bañuelos et al. (2015).

A complete description of the model including the mathematical expressions for the functions described above, parameter values, and initial conditions for each simulation, can be found in the Appendix.

2.2. Numerical simulations

Our model reproduces the activity of several neuronal populations associated with sleep patterns over several sleep/wake cycles. We numerically compute solutions of this model for different values of the parameter T_a describing the ambient temperature and initial conditions taken on the attracting periodic solution at $T_a = 29^\circ$. For our model, $T_a = 29^\circ$ is considered the ideal ambient temperature at which the body uses the minimum energy to thermoregulate, based on ambient temperature values from several studies and prior models (Haskell et al., 1981b). For each solution we calculate the following sleep features: "night length", time asleep, REM latency, number of awakenings, average awakening length, number of REM cycles, and average REM length.

The different sleep features were calculated as follows. The night period is defined as the time from the activation of POAH population ($v_{POAH} > 0$) until the inactivation of POAH population ($v_{POAH} < 0$), not including brief awakenings shorter than a few minutes. Thus, the night length is the duration of the night period. The time asleep is calculated by measuring the difference between the total time spent awake during the night ($v_{POAH} < 0$) and the night length. Since sleep begins with an episode on NREM activity, we measure REM latency as the time from the activation of POAH population ($v_{POAH} > 0$) to the first time the REM-ON population becomes active ($v_{Ron} > 0$). The number of awakenings are calculated by counting the number of times the POAH population becomes inactive during the night period. We also measure the time awake during the night by calculating the amount of time POAH is inactive during the night. Thus, we compute the average awakening length by dividing the total time spent awake during the night by the number of awakenings. A REM cycle consists of a period of NREM activity ($v_{Roff} > 0$) followed by a period of REM activity ($v_{Ron} > 0$).

Finally, the average REM length is calculated by adding the total time spent in each REM bout ($v_{Ron} > 0$) and dividing by the number of REM cycles.

In this paper we present two different types of simulations. First, we compute the solution for a single sleep/wake cycle for different ambient temperatures $T_a \in \{21^\circ, 24^\circ, 29^\circ, 31^\circ, 37^\circ\}$ as it was done in Bañuelos et al. (2015). This set of temperatures is chosen to mimic experimental procedure presented by Haskell et al. (1981a) for which the most experimental data is available. We will refer to this simulation as **Single Night Measurement**. Since in our modified model the temperature has an impact in the REM population, in addition to what was reported in Bañuelos et al. (2015), we are now also reporting the REM latency. The results from this simulation can be found in Table 1. We have chosen to do this simulation in order to compare the behavior of our model with the data obtained by Haskell et al. (1981a).

In the second simulation henceforth referred to as **Fixed Temperature Average**, we compute the solution for thirty sleep/wake cycles where the ambient temperature was fixed at $T_a \in \{21^\circ, 24^\circ, 31^\circ, 37^\circ\}$. That is, we simulate a human subject sleeping in an environment where the ambient temperature is at a constant, non-thermoneutral value ($T_a \neq 29^\circ$) for one month. The results from this simulation are presented in Table 2 and show the measurements of the average of the sleep features described above. The data for the first night was excluded in this average computation to accommodate for transients in the model. The transient behavior seemed to be mostly contained within the first night's data, with the second and subsequent nights all being very similar to each other (comparison not shown) We have chosen to do this simulation in order to investigate the long-term effects of REM deficits caused by sleeping at temperatures away from thermoneutrality. As discussed in Section 4 and motivated by the Energy Allocation Theory (Schmidt, 2014), lack of REM might be the cause of many different pathologies. We believe this study can motivate further experimental questions and protocols.

3. Results

3.1. Results at thermoneutral

We present the sleep features for the solution of our model at $T_a = 29^\circ$ which is considered thermoneutral, that is, without temperature effects (see Fig. 1) and initial conditions on the limit

Table 1
Results of **Single Night Measurement** simulations at various ambient temperatures. The initial conditions are set on the periodic orbit for 29°.

	Temperature (°C)				
	21	24	29	34	37
Night Length (h)	6.40	6.18	7.96	6.64	6.99
Time Asleep (h)	6.21	6.11	7.96	6.46	6.72
REM Latency (min)	116.16	104.10	101.28	115.92	156.18
Num. Awakenings during night	3	1	0	3	3
Avg. Awakening Length (min)	3.88	4.44	n/a	3.56	5.26
Num. REM Cycles	4	4	5	4	4
Avg. REM Length (min)	8.30	11.48	20.33	10.04	4.72

Table 2
Results of **Fixed Temperature Average** simulations. Here the average over 30 nights is computed for the sleep features of night length, REM latency, number of awakenings during night, and number of REM cycles. The data for awakening length, and REM length is averaged over each night and averaged over 30 nights.

	Temperature (°C)				
	21	24	29	34	37
Night Length (h)	7.65	7.54	7.96	7.73	7.78
Time asleep (h)	7.39	7.40	7.96	7.47	7.47
REM Latency (min)	133.37	121.90	101.30	128.71	174.37
Num. Awakenings during night	3.97	1.97	0	3.77	3.53
Avg. Awakening Length (min)	3.90	4.21	n/a	4.04	5.25
Num. REM Cycles	4.97	4.97	5	4.77	4.53
Avg. REM Length (min)	8.35	12.00	20.33	10.05	4.55

cycle. Simulations at this temperature are designed to emulate a typical night of sleep. Parameters are given in Table A.2 and were chosen such that model simulations are consistent with available experimental data concerning human sleep statistics. Our simulations indicate a typical 24-h cycle that consists of 8 h of sleep followed by 16 h of wakefulness (Fig. 2). The 8-h sleep, corresponding to positive v_{POAH} values, consists of periods of both REM and NREM sleep. At thermoneutral, our model exhibits a night length of 7.9 h and consists of 5 REM Cycles averaging 90.3 min in length. This is consistent with findings that indicate that a typical night of human sleep consists of 4-5 REM cycles of about 90–100 min length (Benington and Heller, 1994; Clausen et al., 1974; Rogers and Holmes, 2012). There are a number of more subtle experimental observations that are well replicated by the current model. REM sleep should constitute approximately 20% of sleep. REM stage sleep is not uniformly distributed across the night and REM bouts tend to be longer in the second half of the night (Phillips et al., 2013). Moreover, the first REM bout of the night should be 5–10 min long (Rogers and Holmes, 2012) and occur approximately 100 min into the night (Clausen et al., 1974). Our simulations yield REM to be 20.3% of the night. Simulations exhibit REM bouts that increase from 8 min for the first bout to 36 min for the last with the first REM bout occurring 101 min into the night. Further details of the dynamics of the model can be found in Bañuelos et al. (2015).

3.2. Temperature effects to POAH and REM regulator

There is a circadian rhythm of core body temperature, T_{set} in our model, with an amplitude of about 0.5° around its mean of 37° (grey line in Fig. 3), and humans typically fall asleep during the descending phase of the temperature rhythm (Czeisler et al., 1980b; Zulley et al., 1981). The variable C_t is the circadian potential propensity to fall into REM, which depends on the circadian cycle of the temperature T_b. The variable T_{set} defines the ideal body temperature for all points during a 24-h circadian cycle. In our previous model (Bañuelos et al., 2015), we considered the temperature effects to the temperature-sensitive neurons in the POAH (indicated by the blue dashed bubble and associated arrow of the diagram in Fig. 1). During REM bouts, body temperature T_b, deviates from the target temperature T_{set} as there is an almost complete inability to thermoregulate. When this deviation exceeds a threshold of 0.5°C ($T_b = T_{set} \pm 0.2$), (lower bound indicated by the dashed blue line in Fig. 3 and upper bound indicated by red line in Fig. 3), then an inhibitory pulse is sent to the POAH in order to induce a brief awakening and restore thermoregulation (see Sections 2.5.1 and 3.3 in Bañuelos et al., 2015).

As a main novelty herein we include the effects of temperature on the temperature-dependent REM regulator, causing variations in the REM latency and duration of REM bouts. These effects are indicated in Fig. 1 by the blue dashed inhibitory connection between the POAH and REM-OFF populations. We model these effects by incorporating two different inputs on the temperature-dependent REM regulator, body temperature, T_b, and total metabolic expenditure, m, as we describe below.

The synaptic current from POAH to REM-OFF neurons, $I_{POAH \to Roff}$ includes an additional multiplicative term, syn, which models the propensity to fall into REM and depends mainly on the body temperature (see Eq. (2)). Specifically, this synaptic current takes the form

$$I_{POAH \to Roff} = g_{POAH \to Roff} s_{\infty,v}(v_{POAH}, v_{5,POAH}) syn (v_{Roff} - E_{syn}).$$

When the variable syn reaches a certain critical value ($syn \approx 0.327$), POAH neurons inhibit REM-OFF neurons strongly enough so that oscillations between REM-ON and REM-OFF emerge (see Section 3.2 in Bañuelos et al., 2015). However, the transition to the activation of REM-ON neurons may occur for

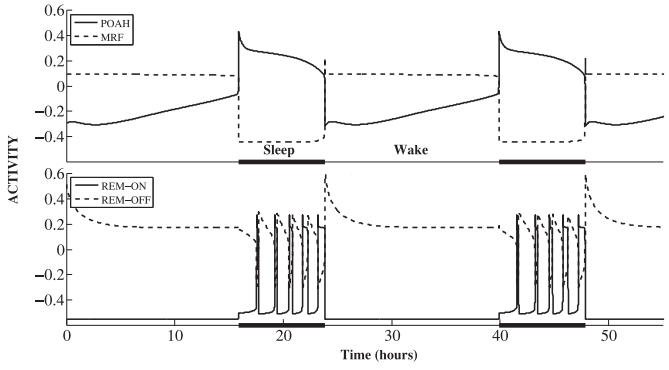

Fig. 2. The activity of various neuron groups during sleep/wake cycling at ambient temperature $T_a = 29°$ (thermoneutral). Periods of sleep are indicated by bold horizontal lines along the x-axis.

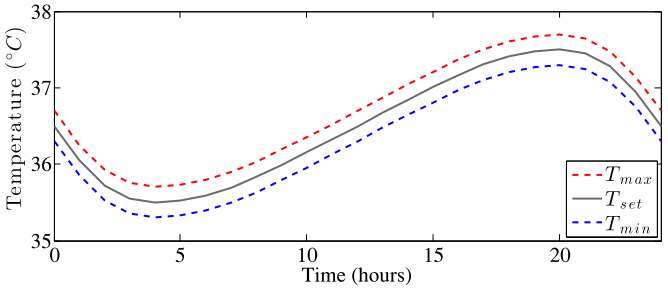

Fig. 3. Ideal body temperature, T_{set}, as set by circadian input. Allowable deviations indicated by dashed lines. The lower bound is indicated by the dashed blue line and the upper bound is indicated by the dashed red line. For interpretation of the references to color in this figure legend, the reader is referred to the Web version of this article.

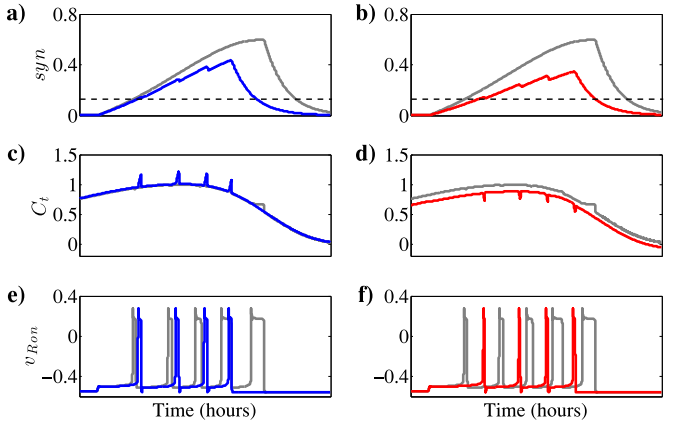

Fig. 4. Time courses of *syn*, C_t, and v_{Ron} over 12 h covering a night cycle for three different temperatures $T_a \in \{21^\circ, 29^\circ, 37^\circ\}$. The left column compares variable values for temperatures cooler than thermoneutral, with $T_a = 29^\circ$ (grey) and $T_a = 21^\circ$ (blue) while the right column displays variable values for temperatures warmer then thermoneutral, with $T_a = 29^\circ$ (grey) and $T_a = 37^\circ$ (red). For interpretation of the references to color in this figure legend, the reader is referred to the Web version of this article.

values of *syn* before the critical value is achieved due to transient effects. In Fig. 4a and b, we show that for values of *syn* around 0.13 (indicated with a horizontal black line) there occurs the first transition to REM corresponding to the activation of the REM-ON population (compare Fig. 4a to e and b to f).

The variable *syn* satisfies the following differential equation:

$$syn' = \frac{(C_t(T_b) - syn)(syn + 0.35)}{\tau_3(m)} H(v_{POAH} - v_{th}) - \frac{syn}{\tau_4} H(v_{th} - v_{POAH}), \quad (2)$$

where

$$C_t(T_b) = 1 - (T_b - 36.5),$$

is the temperature-dependent circadian potential propensity, and

$$\tau_3(m) = 450 + \frac{300}{1 + e^{-(m-10)/2}}. \quad (3)$$

The variable m measures the amount of metabolic processes that the body needs to activate in order to keep the body temperature at the target value T_{set} (see Eq. (A.3)):

$$m = H(T_b - T_{set}) \frac{v_c(T_b - T_{set})}{k_c + (T_b - T_{set})} + H(T_{set} - T_b) \frac{v_h(T_{set} - T_b)}{k_h + (T_{set} - T_b)}.$$

Notice that when the body needs to cool down (warm up, respectively), only the first term (second term, respectively) contributes to the variable m.

Czeisler et al. (1980a) report a particularly close relation between the circadian-modulated core body temperature and the rhythm of REM sleep propensity. We incorporate this idea into our model through the variable C_t, the circadian-mediated propensity to fall into REM, which depends on the circadian cycle of the temperature T_b. During sleep, *syn* will grow towards the value C_t and decay to zero during wake. Thus, as opposed to previous models, we assume here that the propensity to transition into REM sleep depends mainly on the body temperature rather than the amount of time spent in NREM sleep, via the variable C_t. Indeed, C_t oscillates as T_b on a 24-h period but with opposite sign. When the body temperature decays, C_t rises, which is usually at the beginning of the night (see Fig. 4).

Moreover, when the body is using large amounts of energy to keep the body temperature at the target temperature, which happens when T_a is far from thermoneutral (for instance $T_a = 37^\circ$), m is large and so is the variable τ_3 (see Fig. 4, bottom), which controls the time rise of the variable *syn* during sleep time. Therefore the variable *syn* rises more slowly than for $T_a = 29^\circ$ (see Fig. 4, top), causing an increase in the REM latency with respect to thermoneutral. Notice that the activation of V_{Ron} occurs with a certain delay with respect to thermoneutral.

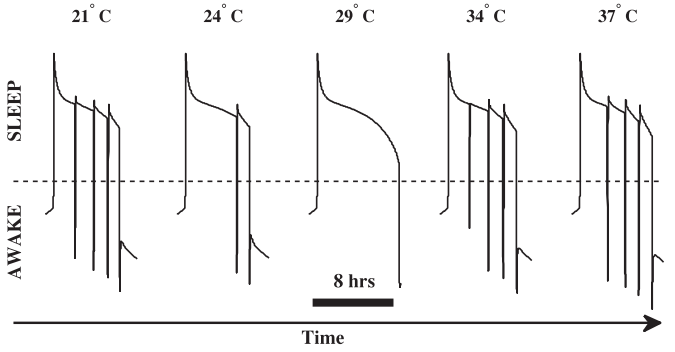

Fig. 5. POAH activity during one night, showing awakenings at various ambient temperature values.

In Fig. 5 we show the time course of v_{POAH} across a single night at the following ambient temperatures: $21^\circ, 24^\circ, 29^\circ, 34^\circ$, and 37°. Awakenings that occur within a night correspond to v_{POAH} dropping into the awake activity range ($v_{POAH} < 0$). When the ambient temperature is thermoneutral (29°), no awakenings occur during the night. As the ambient temperature deviates further from thermoneutral, there is an increased need for thermoregulation throughout the night, and thus an increased number of awakenings per night.

3.3. Model dynamics

Model parameters have been chosen such that, at thermoneutral, the system has a stable limit cycle with a 24-h period (see Tables A.1 and A.2 for parameter values).

More precisely, the variable v_{POAH} over one period remains active ($v_{POAH} > 0$) for 8 h corresponding to sleep and inactive ($v_{POAH} < 0$) for 16 h corresponding to wake.

The introduction of temperature effects on our system alters the behavior of the system in a number of ways. In particular, deviations of body temperature from the acceptable range produce brief awakenings during the night, thus causing changes in the cycle of the variable v_{POAH}.

In Fig. 6, we numerically investigate how the ambient temperature T_a affects the dynamics of this system by looking at the variables describing the activity of the POAH neuronal population. For different temperatures, we look at the values of w_{POAH} when $v_{POAH} = 0$ (Poincaré section at $v_{POAH} = 0$) which correspond to transitions from awake to sleep and vice versa. For ambient temperatures near thermoneutral (between 28° and 31°), model simulations generate no awakenings and the trajectories approach a limit cycle. Crossings occur only at two different values of w_{POAH} corresponding to the onset and termination of sleep (see Fig. 6a). The trajectory projected onto the $v_{POAH} - w_{POAH}$ plane at 29° is shown in Fig. 6c. The closed loop is indicative that the trajectory has approached a limit cycle. For temperatures further away from thermoneutral, the long-term behavior of the system is less clear. Indeed, crossings of the section v_{POAH} occur for several values of w_{POAH} without any detectable pattern (see Fig. 6a). Fig. 6b and d show the trajectories onto the $v_{POAH} - w_{POAH}$ for an extended simulation at 21° and 37°, respectively. While the trajectory remains bounded, the periodicity of the trajectory is difficult to assess. If a stable limit cycle exists in these cases, it must either be weakly

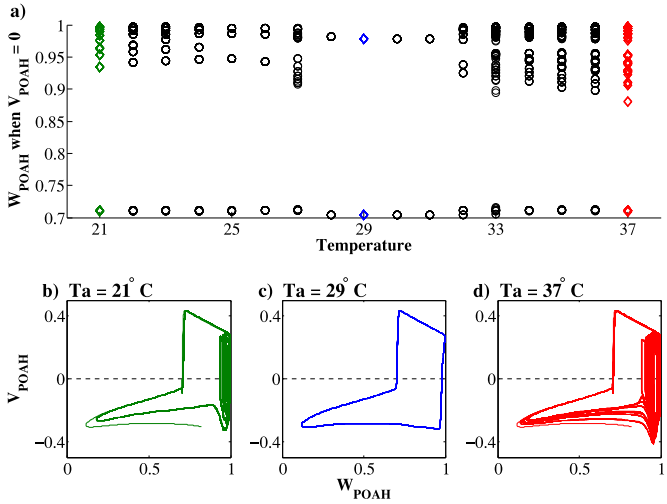

Fig. 6. (a) For different temperatures, we consider the values of w_{POAH} at the times when the POAH activity transitions between active and inactive, i.e. when $v_{POAH} = 0$. Panels (b), (c), and (d) show the activity of the model projected onto the $v_{POAH} - w_{POAH}$ plane, at the ambient temperature $T_a = 21°$, $T_a = 29°$ (thermoneutral), and $T_a = 37°$, respectively. For interpretation of the references to color in this figure legend, the reader is referred to the Web version of this article.

attracting or having a period that is long enough to be difficult to discern from these simulations.

3.4. Simulation results

The **Single Night Measurement** simulation aims at exploring changes in sleep dynamics for a subject who sleeps at an ambient temperature of $T_a \in \{21°, 24°, 29°, 31°, 37°\}$ for one night. As the ambient temperature deviates from thermoneutral, more complicated dynamics are observed (see Table 1). Indeed, our model displays more awakenings at extreme temperatures and the total time awake increases as the ambient temperature moves away from thermoneutral. The average REM length decreases as the ambient temperature moves towards the extreme temperatures with the lowest values of average REM length at $T_a = 21°$ and $T_a = 37°$. In a similar way, the REM latency increases as the ambient temperature deviates from thermoneutral with the largest values of REM latency in the extreme ambient temperatures. Similar to Haskell et al. (1981a) and Muzet et al. (1983), our model produces a quadratic relationship between REM characteristics and distance of ambient temperature away from thermoneutral (Fig. 7). In addition, the night length and the time asleep decrease for non-thermoneutral ambient temperatures (Haskell et al., 1981a; Muzet et al., 1984). Haskell et al. (1981a) report mean observations across several subjects with large variability among subjects. Thus, we aimed for a qualitative alignment with this data.

These observations can be explained by the model. Indeed, our model suspends its thermoregulating functionality while the REM-ON neuronal population is active. When the temperature is set at a drastic value away from 29° and the system has been in REM sleep for too long, the body temperature deviates too far from T_{set}, and an awakening occurs. Thus, awakenings always occur from a period of REM-ON activity and cut short the REM bout. Moreover, when the subject is set to sleep at non-optimal temperatures, more energy is required to keep the body temperature at thermoneutral. This fact requires the system to spend more time in NREM sleep, where it is able to thermoregulate, thus delaying the transition into the first REM bout, and causing a REM latency increase.

The **Fixed Temperature Average** simulation aims at exploring the sleep patterns of a subject who sleeps at a fixed ambient temperature for one month (see Table 2). As noted above, the average

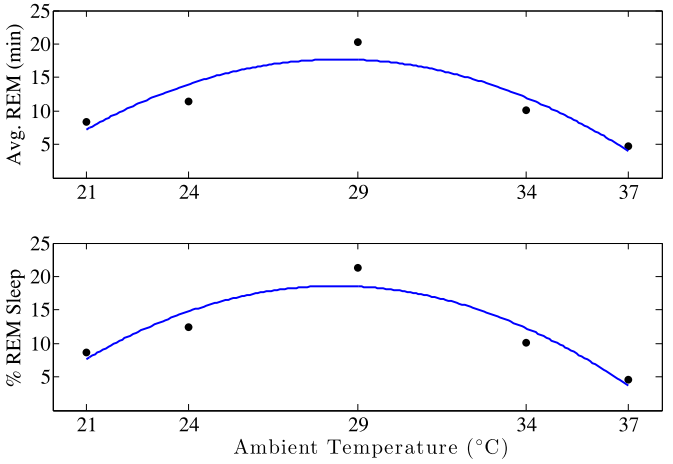

Fig. 7. Quadratic fit of simulated data for average length of REM bouts, and percentage of REM sleep for a single night at $T_a \in \{21°, 24°, 29°, 34°, 37°\}$. Linear fits were also calculated for this data, however, the quadratic fits provide the smallest error.

over the 30 nights was computed for each sleep feature. We observe similar behaviors for the average REM length, the REM latency, and the total time awake as in the **Single Night Measurement** simulation. However, unlike the data in Table 1, the averages of the night length and total time asleep over 30 nights is closer to 8 h. The first night spent at temperatures away from thermoneutral produces very different results for the night length as opposed to allowing the subject to sleep at the same temperature for more nights. Thus, the single night measurements might just be transients as opposed to a more stable solution of the model.

4. Discussion

We have presented a modified and improved model of human sleep/wake regulation that incorporates thermoregulation and the effects of ambient temperature. In Bañuelos et al. (2015), the model displayed features of normal sleep at thermoneutrality in a healthy human adult, such as the timing and duration of sleep, initiating sleep in NREM and waking from REM, and the number and duration of REM cycles. By including the effects of temperature via the temperature-dependent REM regulator, via modulation of POAH – REM-off inhibition, the model presented in this work displays more realistic trends in the REM latency and duration of REM bouts. The implementation of a temperature-dependent REM regulator in the model suggests a plausible mechanism for the functional connectivity between the temperature-dependent and REM-regulating neuronal populations.

The results of two simulations are presented to show the changes on sleep features as the ambient temperature varies. The ambient temperatures under consideration are $T_a \in \{21°, 24°, 29°, 34°, 37°\}$. In Single Night Measurement simulation we compute the solution of the model for 24 h at each ambient temperature. For the Fixed Temperature Average simulation the solution was computed for 30 consecutive nights at each of the five ambient temperatures. Results for the Single Night Measurement and Fixed Temperature Average simulations are presented in Tables 1 and 2, respectively.

As can be observed, the overall length of the night decreases when the ambient temperature in the model is set to temperatures away from thermoneutral. Additionally, nights held at temperatures away from thermoneutral show significantly less time spent in REM sleep and lengthened periods of REM latency.

The REM latency increase in the nights spent at unfavorable temperatures may be due to the increase in energy required to

maintain an appropriate core body temperature. This requires the model to spend more time in NREM sleep, where it is able to thermoregulate, thus delaying the transition into the first REM bout. Similarly, during the night, once in a REM bout, the lack of thermoregulating will cause the body temperature to deviate from its optimal temperature. Once the body becomes too hot or too cold, a brief awakening will occur, disrupting the REM bout, and ultimately the system will fall back into NREM sleep. These disruptions throughout the night lead to a decrease in the overall length of time spent in REM sleep.

Among data in the literature for human sleep there are substantial quantitative differences as well as a conflicting qualitative difference in whether warmer or cooler non-thermoneutral temperatures have a greater impact on REM duration (Haskell et al., 1981a; Muzet et al., 1983). As such, we aim to capture qualitative agreement with experimental results. The Fixed Temperature Average simulation was done as a first step toward answering the question: How might experimental subjects' sleep behavior change if they were sleeping at a particular temperature for many nights and then data were collected? Generally, this is an uncommon set up for experimental sleep studies. So, we hope that our results here and our future modeling efforts aid in determining these long-term effects, perhaps inspiring a new and different direction for experimental studies to pursue. This is experimental data we need in order to improve our model.

While the mathematical model has a simple periodic orbit at 29°, Fig. 6 shows that the orbits may become more complicated at other temperatures. In these cases, the model still showed sleep onset at an appropriate circadian phase, but waking phases and sleep quantities varied as the model had either four or five REM/NREM cycles. Numerically, these quantities varied in a pattern of five days at 34C and seven days for 37° (results not shown); we will investigate the mathematical properties of these orbits in future work. These model dynamics may also have biological significance; in fact, more complex dynamics than anticipated are sometimes observed in experimental sleep protocols. Temperature is only one of many external factors that interact with sleep, and perturbed sleep need not be periodic (McCauley et al., 2009).

Other perturbations are known to lead to altered sleep dynamics. Human subjects living for months in environments shielded from light cues reveal the phenomenon of "internal desynchronization," in which circadian rhythms of sleep and body temperature spontaneously adapt to different periods (see Strogatz et al., 1986 for a review of these studies and models). Our model results suggest that subjects who regularly sleep at temperatures away from thermoneutral may experience altered sleep dynamics as well as reduced quality during sleep.

It has been shown that sleep deprivation and jet lag can affect sleep features like those measured in this paper. Given our model, next steps include incorporating mechanisms for forced periods of awakening and time shifts, which will allow us to investigate the effects energy use and thermoregulation have on sleep behavior in unfavorable scenarios beyond just drastic ambient temperatures. We plan to construct maps similar to those in Booth et al. (2017) at various ambient temperatures to investigate trends in homeostat value at sleep onset.

CRediT authorship contribution statement

Selenne Bañuelos: Conceptualization, Methodology, Software, Formal analysis, Writing - original draft, Writing - review & editing, Visualization. **Janet Best:** Conceptualization, Methodology, Supervision. **Gemma Huguet:** Conceptualization, Methodology, Software, Formal analysis, Writing - original draft, Visualization. **Alicia Prieto-Langarica:** Conceptualization, Methodology, Validation, Writing - original draft, Writing - review & editing. **Pamela B. Pyzza:** Conceptualization, Methodology, Software, Formal analysis, Writing - original draft, Writing - review & editing. **Shelby Wilson:** Conceptualization, Methodology, Software, Formal analysis, Writing - original draft, Writing - review & editing, Visualization.

Acknowledgments

The authors thank Dr. Markus Schmidt at the Ohio Sleep Medicine Institute for all of his guidance and help and the Institute for Mathematics and its Applications for hosting the Workshop for Women in Applied Mathematics (WhAM!). G.H. has been funded by the Spanish grant PGC2018-098676-B-100 AEI/FEDER/UE and the Catalan grant 2017SGR1049 and the RyC project RYC-2014-15866. JB and PP have been supported by the Mathematical Biosciences Institute and the National Science Foundation under Grant DMS 1440386.

Appendix A. Model

Mean activity of each neuronal population:

$$\begin{aligned} v_i' &= -I_{Ca}(v_i) - I_K(v_i, w_i) - I_{leak}(v_i) + I_i - \sum I_{syn} \\ &= g_{ca} m_\infty(v_i)(v_{ca} - v_i) + g_k w_i (v_k - v_i) + g_l (v_l - v_i) + I_i - \sum I_{syn}, \end{aligned} \tag{A.1}$$

$$w_i' = \lambda_\infty(v_i, v_{3,i}, \phi_i, \tau_i)(w_\infty(v_i, v_{3,i}) - w_i), \tag{A.2}$$

with $i = \{POAH, CRF, ORX, MRF, Ron, Roff\}$.

Steady state activation functions:

$$m_\infty(v) = 0.5\left(1 + \tanh\left(\frac{v - v_1}{v_2}\right)\right),$$

$$w_\infty(v, v_3) = 0.5\left(1 + \tanh\left(\frac{v - v_3}{v_4}\right)\right),$$

$$\lambda_\infty(v, v_3, \phi, \tau) = \frac{\phi}{\tau}\cosh\left(\frac{v - v_3}{2v_4}\right).$$

Synaptic currents, generally I_{syn}, from neuronal population i to population j satisfy:

$$I_{syn} = g_{syn} s_\infty(v_i, v_{5,i})\left[v_j - E_{syn}\right],$$

where g_{syn} is the strength of the ij synapse, E_{syn} is the synaptic reversal potential and s_∞ is the activation function given by:

$$s_\infty(v, v_5) = 0.5\left(1 + \tanh\left(\frac{v - v_5}{v_6}\right)\right).$$

The synaptic currents from MRF to POAH, $I_{MRF \to POAH}$, and ORX to POAH, $I_{ORX \to POAH}$, include an additional multiplicative term, syn_b.

$$I_{syn} = g_{syn} syn_b s_\infty(v_i, v_{5,i})[v_j - E_{syn}]$$

where syn_b satisfies

$$syn_b' = \frac{(0.2 - syn_b)}{50} H(v_{POAH} - v_{th}) + \frac{(1 - syn_b)}{100} H(v_{th} - v_{POAH}).$$

This term modulates the strength of the inhibition from MRF and ORX to POAH, so that it is strong during wake but is weakened during sleep. This allows for brief awakenings during sleep. For more detailed information see Section 3.3 in Bañuelos et al. (2015).

The synaptic current from POAH to REM-OFF neurons, $I_{POAH \to Roff}$, includes an additional multiplicative term that models a temperature-dependent REM regulator (See Eq. (A.5) and Section 3.2). For all inhibitory synaptic connections, $E_{syn} = -0.7$. The excitatory synaptic equations, $E_{i \to j}$, and other parameter values can be found in Tables A.1 and A.2. Further, ΣI_{syn} for each pop-

Table A.1
Parameter values for each neuron population. $^{*}\tau_{Roff}$ is described by a function dependent on the potential of the REM-OFF neurons, $\tau_{Roff}(v_{Roff}) = 5 + 35H(v_{Roff} - v_{th})$.

Neuron population	Parameter values				
	$v_{3,i}$	$v_{5,i}$	ϕ_i	I_i	τ_i
POAH	−0.15	0	0.01	0	1
CRF	−0.15	−0.1	0.05	0.7	1
ORX	0.1	−0.1	1	0	1
MRF	0.1	−0.1	1	0	1
REM-ON	0.18	0	0.1	0	0.05
REM-OFF	0	0	0.1	0.7	*

Table A.2
Parameters used in the model for neuron populations and body temperature. $^{*}\tau_3$ is described by a function, Eq. (A.6), dependent on amount of metabolic processes. $^{**}\tau_v$ is described by a function, Eq. (A.4), dependent on the activity of the MRF population.

Parameter	Value	Parameter	Value	Parameter	Value
$g_{CRF\to POAH}$	0.5	$E_{MRF\to Roff}$	0.4	v_k	−0.7
$g_{MRF\to Ron}$	0.5	$E_{CRF\to POAH}$	0	v_l	−0.1
$g_{MRF\to POAH}$	0.5	$E_{ORX\to Roff}$	0	v_{ca}	1
$g_{ORX\to POAH}$	1	$E_{ORX\to MRF}$	0	v_1	−0.01
$g_{POAH\to MRF}$	0.5	τ_1	19000	v_2	0.15
$g_{CRF\to MRF}$	0.2	τ_2	2000	v_4	0.145
$g_{ORX\to MRF}$	1	τ_3	*	v_6	0.1
$g_{Roff\to Ron}$	1.1	τ_4	100	v_7	0.01
$g_{MRF\to CRF}$	1	τ_a	0.1	v_{th}	0
$g_{POAH\to ORX}$	1	τ_d	2	v_{th2}	−0.1
$g_{Ron\to Roff}$	0.2	τ_v	**	g_l	0.5
$g_{POAH\to Roff}$	2.1	τ_r	0.002	g_k	2
$g_{ORX\to Roff}$	0.5	v_c	$12H(-v_{Ron})$	g_{ca}	1.33
$g_{MRF\to Roff}$	0.5	v_h	$20H(-V_{Ron})$	g_{cir}	0.3
g_{Tdev}	1.5	k_c	0.05	g_h	7
E_{syn}	−0.7	T_m	8	k_h	0.01

ulation involves a specific combination of currents with the following forms:

$$\begin{aligned}
POAH:&\quad I_{MRF\to POAH} + I_{CRF\to POAH} + I_{ORX\to POAH} + I_{Tdev} + I_{cir} - I_{hom}\\
CRF:&\quad I_{MRF\to CRF}\\
ORX:&\quad I_{POAH\to ORX} - I_{cir}\\
MRF:&\quad I_{POAH\to MRF} + I_{CRF\to MRF} + I_{ORX\to MRF}\\
REM-ON:&\quad I_{MRF\to Ron} + I_{Roff\to Ron}\\
REM-OFF:&\quad I_{MRF\to Roff} + I_{ORX\to Roff} + I_{Ron\to Roff} + I_{POAH\to Roff}.
\end{aligned}$$

Circadian rhythm: The suprachiasmatic nucleus (SCN) of the hypothalamus acts as an endogenous oscillator generating the circadian rhythm. The input from the SCN to the POAH and ORX populations is modeled as a circadian pacemaker, as in Achermann and Borbély (1994):

$$\begin{aligned}
C(t) = {} & 0.97\sin(\omega t) + 0.22\sin(2\omega t) + 0.07\sin(3\omega t)\\
& + 0.03\sin(4\omega t) + 0.01\sin(5\omega t)
\end{aligned}$$

with $\omega = \frac{2\pi}{24}$. The associated current is $I_{cir}(t) = g_{cir}[C(t) + 1]$ with synaptic coupling strength $g_{cir} = 0.3$. For more information see Section 2.3 in Bañuelos et al. (2015).

Sleep homeostatic process: The homeostatic drive for sleep increases while awake (MRF active) and decreases during sleep (POAH active). The homeostat variable h is modeled by the equation

$$h' = \frac{(1-h)}{\tau_1}H(v_{MRF} - v_{th2}) - \frac{h}{\tau_2}H(v_{th2} - v_{MRF}),$$

where $H(\cdot)$ is the Heaviside step function. The associated homeostatic current is $I_{hom}(h) = g_h h$. For more information see Section 2.3 in Bañuelos et al. (2015).

Body temperature model: Following Nijhout et al. (2014), we model thermoregulation as

$$\begin{aligned}
\frac{1}{\tau_v}T_b' = {} & k(T_a - T_b) + T_m - H(T_b - T_{set})\frac{v_c(T_b - T_{set})}{k_c + (T_b - T_{set})}\\
& + H(T_{set} - T_b)\frac{v_h(T_{set} - T_b)}{k_h + (T_{set} - T_b)},
\end{aligned} \tag{A.3}$$

where T_b is the core body temperature, T_a is the ambient temperature, and T_{set} is the temperature the body is trying to maintain. T_{set} fluctuates a half degree Celsius around 37° according to the circadian rhythm, i.e.

$$T_{set}(t) = 0.5C(t) + 37.$$

The time constant τ_v controls the rate at which T_b approaches the steady state value of A.3, as humans thermoregulate most efficiently during wake and less in sleep. Thus, during wake ($v_{MRF} > 0$), $\tau_v = 1$, and during sleep ($v_{MRF} < 0$), $\tau_v = \tau_r = \frac{1}{500}$. This is modeled by

$$\tau_v = (1 - \tau_r)H(v_{MRF}) + \tau_r. \tag{A.4}$$

For more information on the dynamics of T_b see Section 2.5 in Bañuelos et al. (2015).

Parameters involved in body temperature and thermoregulation processes can be found in Table A.2.

Temperature-dependent REM regulator:

$$I_{POAH\to Roff} = g_{POAH\to Roff}s_{\infty,v}(v_{POAH}, v_{5,POAH})syn(v_{Roff} - E_{syn}), \tag{A.5}$$

where

$$s_{\infty,v}(v, v_5) = 0.5\left(1 + \tanh\left(\frac{v - v_5}{v_7}\right)\right),$$

where syn satisfies

$$syn' = \frac{(C_t - syn)(syn + 0.35)}{\tau_3(m)}H(v_{POAH} - v_{th}) - \frac{syn}{\tau_4}H(v_{th} - v_{POAH})$$

with $C_t = 1 - (T_b - 36.5)$ and

$$\tau_3(m) = 450 + \frac{300}{1 + e^{-(m-10)/2}}. \tag{A.6}$$

Amount of metabolic processes that the body needs to activate in order to keep the body temperature at the set value:

$$m = H(T_b - T_{set})\frac{v_c(T_b - T_{set})}{k_c + (T_b - T_{set})} + H(T_{set} - T_b)\frac{v_h(T_{set} - T_b)}{k_h + (T_{set} - T_b)}.$$

See Section 3.2 for more information.

Brief awakenings: When T_b moves beyond the interval $T_b = T_{set}(t) \pm 0.2$, an inhibitory pulse is sent to the POAH in order to induce a brief awakening and restore thermoregulation (Table A.3). The inhibitory current I_{Tdev} is modeled as the product of a conductance with a voltage difference according to the following equations:

$$I_{Tdev} = g_{Tdev}s_{Tdev}(v_{POAH} - E_{syn}),$$

with

$$s_{Tdev}' = I_{pulse}(1 - s_{Tdev})/\tau_a - s_{Tdev}/\tau_d,$$

Table A.3
Initial conditions for the solutions of the model computed within this paper.

$s =$	0	$v_{MRF} =$	0.094471388	$v_{Ron} =$	−0.55577815
$h =$	0.143040288	$w_{MRF} =$	0.48151898	$w_{Ron} =$	$3.9126666e^{-05}$
$p =$	0.74700922	$v_{POAH} =$	−0.30455175	$v_{Roff} =$	0.52038491
$syn =$	0.540022121	$w_{POAH} =$	0.82238168	$w_{Roff} =$	0.2922668
$T_b =$	37.018871	$v_{CRF} =$	0.24835193	$v_{ORX} =$	0.15769777
$syn_b =$	0.3288932122	$w_{CRF} =$	0.43252662	$w_{ORX} =$	0.6885047

and

$$I_{pulse} = H(T_{\min} - T_b) + H(T_b - T_{\max}),$$

where $T_{\min} = T_{set} - 0.2$ and $T_{\max} = T_{set} + 0.2$. I_{pulse} jumps to 1 whenever T_b falls below T_{min} or reaches above T_{max}. Thus S_{Tdev} rises while $I_{pulse} = 1$ and decays to 0 otherwise. For more information see Section 2.5.1 in Bañuelos et al. (2015).

References

Achermann, P., Borbèly, A., 2003. Mathematical models of sleep regulation. Front. Biosci. 8, 683–693.

Achermann, P., Borbély, A.A., 1994. Simulation of daytime vigilance by the additive interaction of a homeostatic and a circadian process. Biol. Cybern. 71 (2), 115–121.

Avidan, A., 2018. Review of Sleep Medicine, fourth ed Elsevier.

Bañuelos, S., Best, J., Huguet, G., Prieto-Langarica, A., Pyzza, P., Schmidt, M., Wilson, S., 2015. Effects of thermoregulation on human sleep patterns: a mathematical model of sleep–wake cycles with rem–rem subcircuit. In: Jackson, T., Radunskaya, A. (Eds.), Applications of Dynamical Systems in Biology and Medicine. Springer, New York, pp. 123–147.

Bassi, A., Vivaldi, E.A., Ocampo-Garcés, A., 2009. The time course of the probability of transition into and out of REM sleep. Sleep 32 (5), 655–669. doi:10.1093/sleep/32.5.655.

Benington, J.H., Heller, H.C., 1994. Rem-sleep timing is controlled homeostatically by accumulation of rem-sleep propensity in non-rem sleep.. Am. J. Physiol. 266 (6), R1992–2000. doi:10.1152/ajpregu.1994.266.6.R1992.

Booth, V., Xique, I., Diniz Behn, C., 2017. One-dimensional map for the circadian modulation of sleep in a sleep-wake regulatory network model for human sleep. SIAM J. Appl. Dyn. Syst. 16 (2), 1089–1112. doi:10.1137/16M1071328.

Borbély, A.A., Baumann, F., Brandeis, D., Strauch, I., Lehman*, D., 1981. Sleep deprivation: effect on sleep stages and EEG power density in man. Electroencephal. Clin. Neurophysiol. 51 (5), 483–493.

Boulant, J.A., 2006. Neuronal basis of Hammel's model for set-point thermoregulation. J. Appl. Physiol. 100 (4), 1347–1354.

Carskadon, M.A., Dement, W.C., 2011. Principles and Practice of Sleep Medicine, fifth ed Elsevier Saunders.

Charkoudian, N., 2003. Skin blood flow in adult human thermoregulation: how it works, when it does not, and why. Mayo Clin. Proc. 78 (5), 603–612.

Cheshire, W.P., 2016. Thermoregulatory disorders and illness related to heat and cold stress. Autonomic Neuroscience 196, 91–104. doi:10.1016/j.autneu.2016.01.001. SI:Thermoregulation.

Clausen, J., Sersen, E.A., Lidsky, A., 1974. Variability of sleep measures in normal subjects. Psychophysiology 11 (4), 509–516. doi:10.1111/j.1469-8986.1974.tb00580.x.

Czeisler, C.A., Weitzman, E.D., Moore-Ede, M.C., Zimmerman, J.C., Knauer, R.S., 1980. Human sleep: Its duration and organization depend on its circadian phase. Science 210 (4475), 1264–1267. doi:10.1126/science.7434029.

Czeisler, C.A., Zimmerman, J.C., Ronda, J.M., Moore-Ede, M.C., Weitzman, E.D., 1980. Timing of REM sleep is coupled to the circadian rhythm of body temperature in man.. Sleep 2 (3), 329–346. doi:10.1093/sleep/2.3.329.

Harding, E.C., Franks, N.P., Wisden, W., 2019. The temperature dependence of sleep. Front. Neurosci. 13.

Harrison, Y., Horne, J., 2000. The impact of sleep deprivation on decision making: areview. J. Exp. Psychol. 6 (3), 236–249.

Haskell, E., Palca, J., Walker, J., Berger, R., Heller, H., 1981. The effects of high and low ambient temperatures on human sleep stages. Electroencephalo. Clin.Neurophysiol. 51 (5), 494–501.

Haskell, E.H., Palca, J.W., Walker, J.M., Berger, R.J., Heller, H.C., 1981. Metabolism and thermoregulation during stages of sleep in humans exposed to heat and cold. J. Appl. Physiol. 51 (4), 948–954.

Imeri, L., Opp, M.R., 2009. How (and why) the immune system makes us sleep. Nat. Rev. 10 (3), 199–210.

Knott, M., Derak, C., McAughery, L., Mehrotra, R., Roudbarani, F., 2017. Sleep deprivation impairs productivity in adults with mood disorders: a scoping review. Am. J. Occup. Ther. 71.

Kumar, R., Bose, A., Mallick, B., 2012. A mathematical model towards understanding the mechanism of neural regulations of wake-NREM-REM states. PLoS ONE 7 (8).

McCauley, P., Kalachev, L.V., Smith, A.D., Belenky, G., Dinges, D.F., Van Dongen, H.P.A., 2009. A new mathematical model for the homeostatic effects of sleep loss on neurobehavioral performance. J. Theor. Biol. 256, 227–239.

Morris, C., Lecar, H., 1981. Voltage oscillations in the barnacle giant muscle fiber. Biophys. J. 35 (1), 193–213. doi:10.1016/S0006-3495(81)84782-0.

Muzet, A., Ehrhart, J., Candas, V., Libert, J.P., Vogt, J.J., 1983. Rem sleep and ambient temperature in man. Int. J. Neurosci. 18 (1–2), 117–125. doi:10.3109/00207458308985885.

Muzet, A., Libert, J.-P., Candas, V., 1984. Ambient temperature and human sleep. Experientia 40 (5), 425–429. doi:10.1007/BF01952376.

Nijhout, H.F., Best, J., Reed, M.C., 2014. Escape from homeostasis. Math. Biosci. 257, 104–110.

Pasula, E., Brown, G., McKenna, B., Mellor, A., Turner, T., Anderson, C., Drummond, S., 2018. Effects of sleep deprivation on component processes of working memory in younger and older adults. Sleep 41.

Phillips, A.J., Robinson, P.A., Klerman, E.B., 2013. Arousal state feedback as a potential physiological generator of the ultradian REM/NREM sleep cycle. J. Theor. Biol. 319, 75–87. doi:10.1016/j.jtbi.2012.11.029.

Rogers, L., Holmes, M., 2012. Model of the Human Sleep Wake System. arXiv:1208.3228v1.

Romanovsky, A.A., 2007. Thermoregulation: some concepts have changed. Functional architecture of the thermoregulatory system. Am. J. Physiol. 292 (1), R37–R46.

Romeijn, N., Verweij, I., Koeleman, A., 2012. Cold hands, warm feet: sleep deprivation disrupts thermoregulation and its association with vigilance. Sleep 35 (12), 1673–1683.

Schmidt, M.H., 2014. The energy allocation function of sleep: a unifying theory of sleep, torpor and continuous wakefulness. Neurosci. Biobehav. Rev. 47, 122–153.

Schmidt, M.H., Swang, T.W., Hamilton, I.M., Best, J.A., 2017. State-dependent metabolic partitioning and energy conservation: a theoretical framework for understanding the function of sleep. PLoS ONE 12 (10).

Shapiro, C.M., Goll, C.C., Cohen, G.R., Oswald, I., 1984. Heat production during sleep. J. Appl. Physiol. 56, 671–677.

Siegel, J.M., 2005. Clues to the function of mammalian sleep. Nature 437.

Strogatz, S.H., Kronauer, R.E., Czeisler, C.A., 1986. Circadian regulation dominates homeostatic control of sleep length and prior wake length in humans. Sleep 9 (2), 353–364.

Tarawah, R., 2017. The relation between sleep deprivation and metabolic syndrome. Int. J. Med. Health Res. 3.

Van Someren, E., 2006. Mechanisms and functions of coupling between sleep and temperature rhythms. Progr. Brain Res. 153, 309–324.

Zulley, J., Wever, R., Aschoff, J., 1981. The dependence of onset and duration of sleep on thecircadian rhythm of rectal temperature. Pflugers Arch. 391 (4), 314–318. doi:10.1007/BF00581514.